Second-Harmonic Generation in OP-GaAs0.75P0.25 Heteroepitaxially-Grown from the Vapor Phase

Journal:	*CrystEngComm*
Manuscript ID	CE-COM-12-2024-001304.R1
Article Type:	Communication
Date Submitted by the Author:	06-Feb-2025
Complete List of Authors:	Wang, Li; Max-Born-Institut fur Nichtlineare Optik und Kurzzeitspektroskopie im Forschungsverbund Berlin eV Vangala, Shivashankar; AFRL Popien, Stefan; APE Angewandte Physik & Elektronik GmbH Beutler, Marcus; APE Angewandte Physik & Elektronik GmbH Mann, James; Air Force Research Laboratory, Sensors Directorate Tassev, Vladimir; Air Force Research Laboratory Büttner, Edlef; APE Angewandte Physik & Elektronik GmbH Petrov, Valentin; Max-Born-Institut fur Nichtlineare Optik und Kurzzeitspektroskopie im Forschungsverbund Berlin eV

Second-Harmonic Generation in OP-$GaAs_{0.75}P_{0.25}$ Heteroepitaxially-Grown from the Vapor Phase

Li Wang,[1] Shivashankar R. Vangala,[2] Stefan Popien,[3] Marcus Beutler,[3] J. Matthew Mann,[2] Vladimir L. Tassev,[2] Edlef Büttner,[3] Valentin Petrov[1,*]

[1]Max-Born-Institute for Nonlinear Optics and Ultrafast Spectroscopy, Max-Born-Str. 2A, 12489 Berlin, Germany

[2]Air Force Research Laboratory, Wright Patterson AFB, OH 45433, USA

[3]APE Angewandte Physik und Elektronik GmbH, Plauener Str. 163-165, Haus N, 13053 Berlin, Germany

**petrov@mbi-berlin.de*

Abstract: Second-harmonic generation using femtosecond pulses at 5.5 µm with a repetition rate of 80 MHz is demonstrated in □500-µm thick layers of orientation-patterned $GaAs_{0.75}P_{0.25}$ grown by hydride vapor phase epitaxy on a structured GaAs template. The length of the sample used (□500 µm) corresponds to only 4 quasi-phase matching periods of 8 coherence lengths.

1. Introduction

Numerous applications in spectroscopy, sensing, telecommunications, chemistry, biology, medicine, and defense demand compact and tunable coherent sources emitting above 5 μm, an upper wavelength limit for direct solid-state laser systems (e.g., Fe^{2+}-doped chalcogenides) and simultaneously an upper transparency limit for oxide based nonlinear crystals such as birefringent or periodically-poled $LiNbO_3$ that can be used for parametric frequency down-conversion of mature diode-pumped laser sources operating in the near-IR between 1 and 3 μm. Since non-oxide nonlinear optical crystals do not exhibit ferroelectric properties for electric-field poling, periodic structures with alternating crystal polarity have been fabricated by orientation-patterned (OP) epitaxial growth from the vapor phase. This presents a viable solution for frequency down-conversion via quasi-phase matching (QPM) which is free of spatial walk-off [1]. The most successful of the binary III-V semiconductors with cubic but non-centrosymmetric zinc-blende ($F\bar{4}3m$) symmetry that have been applied for manufacturing such structures was GaAs [2], which combines superior second-order nonlinearity and thermal conductivity with transparency up to 18 μm. However, GaAs suffers from two-photon absorption (TPA) up to 1.7 μm and for this reason cannot be pumped by well-established, pulsed laser sources below this wavelength [3]. Since this limitation is related to the band-gap energy E_g, the wider band-gap GaP (E_g = 2.35 eV) has been studied as an alternative solution to avoid such TPA. Apart from extending the transparency to shorter wavelengths, the larger band-gap energy of GaP leads to lower refractive index, higher thermal conductivity at lower thermal expansion, and higher optical damage resistivity and hardness [4]. On the negative side, the increased band-gap is associated with lower nonlinearity and lower upper transparency limit in the mid-IR [1,5]. All relevant properties for a specific three-wave nonlinear process, however, can be engineered by growing ternary OP structures of $GaAs_{1-x}P_x$ by heteroepitaxy [6-8]. The preferable substrate in this case is GaAs due to the better availability of high quality wafers at lower price compared to GaP and the maturity of the template preparation process. In [9] we demonstrated the first nonlinear frequency conversion (second-harmonic generation, SHG) in such a ternary OP-GaAsP structure with a nominal P content of x = 15%, i.e. OP-$GaAs_{0.85}P_{0.15}$, grown on an OP-GaAs template. Increasing the P-content is, however, instrumental for finding niche applications for such ternary periodic structures in QPM frequency conversion in the mid-IR part of the spectrum and SHG is the ultimate test of the optical and structuring quality achieved. Here, we report on successful SHG in OP-$GaAs_{0.75}P_{0.25}$ which is suitable for pumping by 1.56 µm Er-fiber laser systems, including ultrafast, for down-conversion to the mid-IR beyond 5 µm without TPA.

2. Results and discussion

The ternary OP structures were grown by low-pressure Hydride Vapor Phase Epitaxy (HVPE) in a horizontal quartz tube reactor using □500-µm thick OP-GaAs templates [8]. The OP-GaAs templates employed were fabricated at BAE Systems (Nashua, NH) by Molecular Beam Epitaxy (MBE) assisted polarity inversion on 500-µm-thick standard (001) GaAs wafers with a 4° miscut towards the [111]B direction and domain walls parallel to the (110) surfaces [10]. The reactor pressure was 3.8 Torr, the substrate temperature was 726˚C, and the total gas flow was 320 sccm. Molten Ga overflown by HCl diluted with hydrogen (H_2) to form GaCl and a mixture of AsH_3+PH_3 diluted with H_2 served as group-III and group-V precursors, respectively. For the targeted epitaxial layer composition with x = 0.25, the PH_3 flow rate was 64 sccm, much higher compared to the AsH_3 flow of 19 sccm, to account for the higher volatility of P compared to As [8]. The growth of the □500 µm thick ternary structured layer took □12 h at an average growth rate of 42 µm/h and the total thickness (template + grown layer) reached □1 mm, cf. Fig. 1(b).

We used a quarter of the 3-inch OP-GaAs template to fabricate OP-$GaAs_{0.75}P_{0.25}$ layers of eight different periods as shown in Fig. 1(a). Seven of them were designed for parametric down-conversion from 1.56 µm to the 6 - 14 µm range, i.e. covering the entire transparency range of the material [4]. Note, that the P-content x = 25% is kept to the minimum that ensures TPA is absent at 1.56 µm (with some reserve) and simultaneously maintains a maximized nonlinear coefficient d_{14} for the mixture. The actual P-content was confirmed by X-ray diffraction and photoluminescence methods. The variation along the growth direction was estimated to be less than 1 % for the first 500 µm of growth [11].

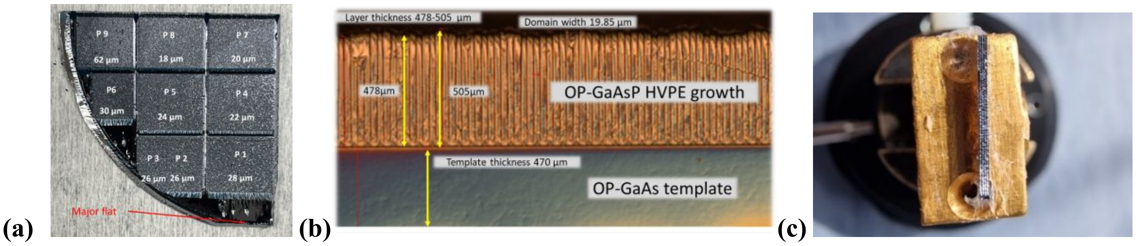

Fig. 1. The quarter wafer with heteroepitaxially grown structured layers of $GaAs_{0.75}P_{0.25}$ of eight different (as indicated) domain thicknesses (a), a cross-section of a sample from part P 7 (b), and top view of sample P 9.2 with a domain width of 62 µm mounted for SHG after down polishing it to a propagation length of □500 µm (c).

`

Figure 1(b) shows a cross section photograph after etching [8] a sample from part P 7. The domain walls are perpendicular to the wafer major flat. Only the part P 9 was structured for SHG to test the overall optical quality achieved for this composition. The chosen domain width of 62 µm corresponds to a fundamental wavelength of 5.423 µm for SHG at 295 K, estimated by averaging the linear susceptibilities (proportional to the square of the refractive indices) and the thermal expansion coefficients of GaAs and GaP [12,13]. To accommodate the large bandwidth of femtosecond pulses, the samples from this part were first cut to a length of 2 mm in the propagation direction and then down-polished by a chemical method to □500 µm with a roughness of 0.8 nm (Impex HighTech GmbH, Germany). As can be seen from Fig. 1(c) the final □500-µm length contains □4 periods of $\Lambda = 124$ µm. The samples were □10-mm wide and □1-mm high (a dimension corresponding to the total thickness of □1 mm in the growth direction).

The fundamental radiation near 5.5 µm for the SHG experiments was derived from difference-frequency generation (DFG) of a commercial synchronously pumped optical parametric oscillator (SPOPO): Levante IR fs with HarmoniXX DFG (APE GmbH, Germany), operating at 80 MHz. With a measured duration of ~130 fs (FWHM) and a spectral width of 346 nm the fundamental pulses were almost bandwidth-limited (Gaussian temporal and spectral profiles assumed), cf. Fig. 2(a). The DFG beam was focused by an uncoated $f = 36$ mm CaF_2 lens to a waist of 280 × 310 µm^2 (e^{-2} metric diameters in the horizontal, i.e. along the □10-mm sample width, and vertical, i.e. along the sample total thickness of □1 mm, directions, respectively). The incident power was adjustable by a waveplate present in the DFG module. The residual fundamental behind the sample was removed by a 2-mm thick absorbing Infrasil plate.

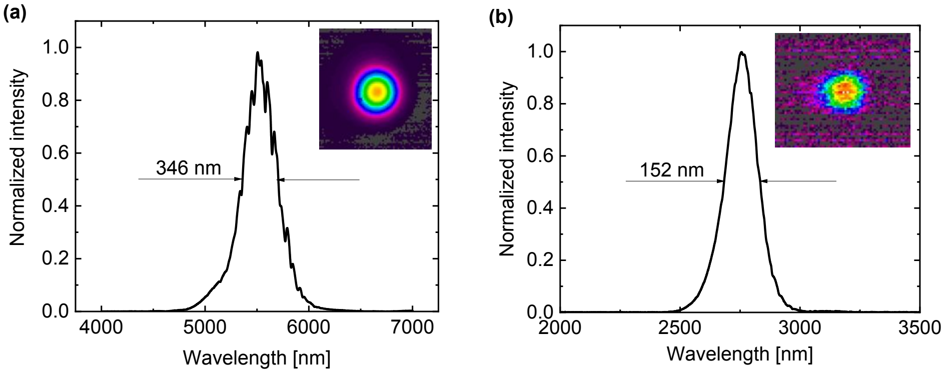

Fig. 2. Fundamental (a) and SH (b) spectra measured using an FT-IR spectrometer (ARCoptix, Switzerland). The insets show the recorded far field beam profiles using Pyrocam PY-III-HR (Ophir-Spiricon, USA) beam profiler.

`

With the fundamental beam polarized in the horizontal plane the effective nonlinearity for QPM is given by $d_{\mathrm{eff}} = (2/\pi)d_{14}$ for second harmonic (SH) polarized in the perpendicular (i.e. vertical) direction.

The measured SH spectrum, Fig. 2(b), had a bandwidth of 152 nm (FWHM), corresponding to Fourier limited pulses with a duration of 74 fs. The temporal walk-off length for a fundamental pulse duration of 130 fs, calculated from the corresponding group velocities in $GaAs_{0.75}P_{0.25}$ based on [12,13] amounts to 0.96 mm. Thus, the pulse shortening of the SH is justified by the squared intensity dependence of the conversion efficiency at low walk-off.

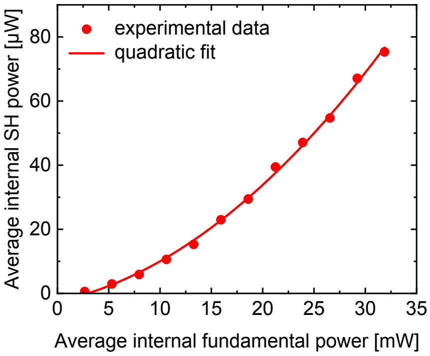

Fig. 3. Average SH power versus average fundamental power at 80 MHz. Both represent internal values after corrections for the Fresnel reflections of the uncoated $GaAs_{0.75}P_{0.25}$ sample.

Only the maximum average SH power could be reliably measured with a power meter. To record the input-output dependence in Fig. 3 we used a calibrated photodiode and lock-in modulation – amplification technique. This figure presents the internal values. An external SH average power of 48.5 µW was measured at the maximum incident pump power of 48 mW for the fundamental at 80 MHz. Taking into account the 89.5% SH transmission of the Infrasil plate and the Fresnel reflections for the uncoated OP-$GaAs_{0.75}P_{0.25}$ sample, the maximum internal SHG conversion efficiency was calculated to be ~0.24%.

The obtained maximum efficiency can be used to evaluate the effective nonlinearity of the SHG process and the nonlinear coefficient d_{14} for $GaAs_{0.75}P_{0.25}$. Usually such values serve as a criterion for the quality of the QPM structures. Using the plane-wave expression for QPM [14] with the spatially averaged intensity for the fundamental wave (equal to half the peak on-axis value for Gaussian beams), we obtained d_{14} = 93 pm/V. This estimate correlates well with the literature values for GaAs [1], converted from SHG at 5.3 μm (CO_2 laser) to the present experiment at 2.75 μm (94-97 pm/V).

Finally we recorded the collimated beam profiles using a pyrocamera (insets in Fig. 2). Although the low average power at the SH was just at the sensitivity limit of the detector array it can be seen that the good beam quality is maintained in the SHG process which is free of spatial walk-off.

3. Conclusion

As depicted in Fig. 1(a), on the same structured OP-GaAs quarter wafer template we have simultaneously grown OP-$GaAs_{0.75}P_{0.25}$ samples with domain widths varying from 18 to 30 μm. We plan to employ such samples in a mid-IR SPOPO for frequency conversion of a mode-locked femtosecond Er-fiber laser at 1.56 μm. The number of quasi-phase matching periods within the same propagation length of □500 μm will be 2 to 3.5 times higher in this case. The same frequency conversion process can be obviously realized with binary OP-GaP. However, the effective nonlinearity of $GaAs_{0.75}P_{0.25}$ is expected to be much higher. While direct estimations of the nonlinear coefficient d_{14} for ternary crystals are missing, compilation of literature data for the same interaction process shows that the nonlinear coefficient of GaP is about 2.3 times lower than that of GaAs [1]. In addition, since OP-GaP is also preferentially grown by heteroepitaxy on GaAs templates [6], the lattice mismatch will be much larger in this case, reaching 3.6%.

References

[1] V. Petrov, Frequency down-conversion of solid-state laser sources to the mid-infrared spectral range using non-oxide nonlinear crystals, Prog. Quantum Electron. 42 (2015) 1-106.

[2] P. S. Kuo, M. M. Fejer, Microstructured semiconductors for mid-infrared nonlinear optics, Ch. 4 in NATO Science for Peace and Security Series - B: Physics and Biophysics, Mid-Infrared Coherent Sources and Applications, pp. 149-168, Eds: M. Ebrahim-Zadeh, I. Sorokina, (Springer, 2007).

[3] P. G. Schunemann, K. T. Zawilski, L. A. Pomeranz, D. J. Creeden, P. A. Budni, Advances in nonlinear optical crystals for mid-infrared coherent sources, J. Opt. Soc. Am. B 33 (2016) D36-D43.

[4] P. G. Schunemann, K. T. Zawilski, T. Lobay, B. Porth, M. D. Thomas, Laser damage threshold study of ZGP, CSP, GaAs, and GaP, Proc. SPIE PC12405 (2023) PC124050G.

[5] V. Petrov, L. Wang, G. Exner, S. R. Vangala, A. Grigorov, E. Ivanova, P. G. Schunemann, V. L. Tassev, Transmission and nanohardness studies of ternary $GaAs_{1-x}P_x$ layers grown from the vapor phase by heteroepitaxy, Opt. Mater.: X 22 (2004) 100313.

`

[6] V. L. Tassev, S. R. Vangala, R. D. Peterson, M. M. Kimani, M. Snure, R. W. Stites, S. Guha, J. E. Slagle, T. R. Ensley, A. A. Syed, I. V. Markov, Heteroepitaxial growth of OPGaP on OPGaAs for frequency conversion in the IR and THz, Opt. Mater. Express 6 (2016) 1724-1737.

[7] V. L. Tassev, S. R. Vangala, D. Tomich, C. Dass, Heteroepitaxial growth of nonlinear optical materials for frequency conversion in the mid and longwave IR, J. Cryst Growth 522 (2019) 210-213.

[8] V. Tassev, S. Vangala, D. Brinegar, M. Parker, T. Barlow, Thick heteroepitaxy of binary and ternary semiconductor materials for nonlinear frequency conversion in the mid and longwave infrared region, Phys. Stat. Sol. A 218 (2021) 2000443.

[9] L. Wang, S. R. Vangala, S. Popien, M. Beutler, V. L. Tassev, V. Petrov, Second-harmonic generation in heteroepitaxially grown, orientation-patterned, ternary GaAsP periodic structures, Phys. Stat. Sol. RRL 16 (2022) 2200198.

[10] C. Lynch, D. F. Bliss, T. Zens, A. Lin, J. S. Harris, P. S. Kuo, M. M. Fejer, Growth of mm-thick orientation-patterned GaAs for IR and THz generation, J. Cryst. Growth 310, (2008) 5241-5247.

[11] V. Petrov, L. Wang, S. R. Vangala, V. L. Tassev, Transmission and absorption measurements of GaAsP layers grown from the vapor phase, Proc. SPIE 11985 (2022) 1198506.

[12] T. Skauli, P. S. Kuo, K. L. Vodopyanov, T. J. Pinguet, O. Levi, L. A. Eyres, J. S. Harris, M. M. Fejer, B. Gerard, L. Becouarn, E. Lallier, Improved dispersion relations for GaAs and applications to nonlinear optics, J. Appl. Phys. 94 (2003) 6447-6455.

[13] J. Wei, J. M. Murray, J. O. Barnes, D. M. Krein, P. G. Schunemann, S. Guha, Temperature dependent Sellmeier equation for the refractive index of GaP, Opt. Mater. Express 8 (2018) 485-490.

[14] R. L. Sunderland, Handbook of Nonlinear Optics, 2nd Edition (Marcel Dekker, 2003).

Funding

This work has been supported by the Air Force Office of Scientific Research (AFOSR), Award # FA8655-20-1-7053.

Author Contributions

Li Wang (Investigation, Methodology, Validation), Shivashankar R. Vangala (Resources), Stefan Popien (Methodology, Formal analysis), Marcus Beutler (Methodology, Validation), J. Matthew Mann (Resources), Vladimir L. Tassev (Resources, Funding acquisition, Methodology), Edlef Büttner (Methodology, Project administration), and Valentin Petrov (Funding acquisition, Investigation, Methodology, Project administration, Supervision, Validation, Writing – original draft, Writing – review & editing).

Competing Interests

The authors have no relevant financial or non-financial interests to disclose.

`

Data Availability Statement

The data analysis scripts of this article are available at

https://drive.google.com/drive/folders/1AxhHcX_veb4LpeAlPaUt4J44Hr3KG64H?usp=drive_link

Data Availability Statement

The data analysis scripts of this article are available at https://drive.google.com/drive/folders/1AxhHcX_veb4LpeAlPaUt4J44Hr3KG64H?usp=drive_link